# UWL REPOSITORY

## repository.uwl.ac.uk

Vertebroplasty: only small cement volumes are required to normalize stress distributions on the vertebral bodies

Luo, Jin ORCID logoORCID: https://orcid.org/0000-0001-5451-9535, Daines, L, Charalambous, A, Adams, MA, Annesley-Williams, DJ and Dolan, P (2009) Vertebroplasty: only small cement volumes are required to normalize stress distributions on the vertebral bodies. Spine, 34 (26). pp. 2865-2873. ISSN 0362-2436

**This is the Accepted Version of the final output.**

**UWL repository link:** https://repository.uwl.ac.uk/id/eprint/6915/

**Alternative formats**: If you require this document in an alternative format, please contact: open.research@uwl.ac.uk

# Vertebroplasty: only small cement volumes are required to normalise stress distributions on the vertebral bodies.

Jin Luo, Luke Daines, Alexander Charalambous, Michael A Adams,

\*Deborah J Annesley-Williams, Patricia Dolan

Department of Anatomy, University of Bristol, Bristol, U.K.

\*Department of Neuroradiology, Queen's Medical Centre, Nottingham, U.K.

**Corresponding author:**

Dr Patricia Dolan, Reader in Biomechanics,

Department of Anatomy, University of Bristol,

Southwell Street, Bristol BS2 8EJ,  U.K.

Trish.Dolan@bris.ac.uk

Tel: +44 (0) 117 9288363

Fax: +44 (0) 117 9254794

**ABSTRACT**

**Study Design.** Biomechanical study of vertebroplasty in cadaver motion segments.

**Objectives**. To determine how the volume of injected cement influences: a) stress distributions on fractured and adjacent vertebral bodies, b) load-sharing between the vertebral bodies and neural arch, and c) cement leakage.

**Summary of Background Data.** Vertebroplasty is increasingly used to treat vertebral fractures, but there are problems concerning adjacent level fracture and cement leakage, both of which may depend on the volume of injected cement.

**Methods:** Nineteen thoracolumbar motion segments from 13 cadavers (42-91 yrs) were loaded to induce fracture. Fractured vertebrae received two sequential injections (VP1 and VP2) of 3.5cm$^3$ of polymethylmethacrylate cement. Before and after each intervention, motion segment stiffness was measured in compression and in bending, and "stress profilometry" was used to quantify the distribution of compressive stress in the intervertebral disc (which presses equally on fractured and adjacent vertebrae). Stress profiles were obtained by pulling a pressure transducer through the disc while the motion segment was compressed in flexed and extended postures. Stress profiles yielded the intradiscal pressure (IDP), the magnitude of stress peaks in the anterior (SP$_A$) and posterior (SP$_P$) annulus, and the % of the applied compressive force resisted by the neural arch (F$_N$). Cement leakage and vertebral body volume were quantified using water-immersion, and % cement fill was estimated.

**Results:** Bending and compressive stiffness fell by 37% and 50% respectively following fracture, and were restored only after VP2. Depending on posture, IDP fell by 59%-85% after fracture whereas SP$_P$ increased by 107%-362%. VP1 restored IDP and SP$_P$ to prefracture values, and VP2 produced no further changes. Fracture

increased $F_N$ from 11% to 39% in flexion, and from 33% to 59% in extension. $F_N$ was restored towards pre-fracture values only after VP2. Cement leakage increased after VP2 and was negatively correlated to vertebral body volume. Following VP2, increases in IDP and compressive stiffness were proportional to % fill.

**Conclusions:** 3.5cm$^3$ of PMMA largely restored normal stress distributions to fractured and adjacent vertebral bodies, but 7cm$^3$ were required to restore motion segment stiffness and load-sharing between the vertebral bodies and neural arch. Cement leakage, IDP and compressive stiffness all increased with % fill.

**Key words:** Vertebroplasty, cement volume, load-sharing, intradiscal pressure, vertebral fracture.

**Mini abstract**

Cadaver motion segments were fractured and treated with two 3.5ml injections of PMMA cement. The first injection largely restored distributions of compressive stress acting on the fractured and adjacent vertebral bodies. However the second injection was required to restore motion segment stiffness, and load-sharing between the vertebral body and neural arch.

**Key points:**

- Clinical studies suggest that large cement volumes during vertebroplasty can increase the risk of adjacent level fracture, and of cement leakage.

- In cadaveric motion segments, a single injection of $3.5cm^3$ of PMMA cement (which gave a mean volumetric fill of approx 13%) largely restored the distribution of compressive stress acting on the fractured and adjacent vertebral bodies.

- Injection of a further $3.5 \, cm^3$ of PMMA (which resulted in a mean volumetric fill of approx 25%) had no further effect on these stress distributions, but it increased motion segment stiffness in bending and in compression. The $2^{nd}$ injection was also required to restore compressive load-sharing between the vertebral body and neural arch.

- The incidence and average volume of cement leakage more than doubled following the second injection, and were greater in small vertebral bodies.

- Small cement volumes can restore normal stress distributions on the vertebral bodies, and minimise cement leakage, but larger volumes are required to restore spinal stiffness and to normalise load-sharing between the vertebral body and neural arch.

## Introduction

Vertebroplasty is a minimally-invasive technique that involves the percutaneous injection of bone cement into unstable or fractured vertebrae in order to strengthen and stabilise them [1]. In recent years, it has been used increasingly in the treatment of osteoporotic vertebral fracture where it has proved effective in alleviating pain [2-6] and improving functional mobility [7]. However, despite the clinical success of the procedure, several potential problems remain, including cement leakage and increased risk of adjacent vertebral fracture.

Clinical studies report highly variable incidence rates for cement leakage, from 22% to 88% of treated levels [8, 9]. A survey of 159 vertebroplasty patients suggests that cement leakage is largely determined by vertebral size and injection volume [10], although factors such as cement viscosity [11-13] and delivery mechanism [10, 13, 14] may also contribute. Cement leakage does not usually cause overt clinical problems, and patients remain asymptomatic [6], but in a small percentage of patients it can cause serious complications such as paraplegia [15], or pulmonary embolism [16, 17].

Adjacent level fracture following vertebroplasty has been reported in many studies [18-22] and may indicate abnormal loading of the non-augmented vertebral body. However, adjacent-level fracture can also reflect systemic weakening of bone in an osteoporotic spine, and the direct influence of cement augmentation remains uncertain. Studies on cadaveric motion segments suggest that vertebral body fracture has a profound effect on the internal mechanical functioning of the adjacent intervertebral disc, and this has consequences for both the fractured and adjacent vertebral bodies because they are both loaded by the disc that lies between them. Vertebral body fracture decompresses the nucleus of the adjacent disc, and generates high concentrations of compressive stress in the posterior annulus, and on the neural arch [23, 24]. Vertebroplasty helps to reverse these effects and largely restores normal

1

compressive load-sharing between the anterior column (vertebral bodies and discs) and the posterior column (neural arches) [25, 26]. Too much cement, however, could elevate intradiscal pressure and increase end-plate deformation in the adjacent vertebral body to such an extent that the risk of adjacent level fracture is increased. [27, 28] Cement leakage into the disc space could further increase loading on the opposing endplate, which may explain why this appears to increase the risk of adjacent level fracture in patients [29, 30].

It appears therefore that large volumes of injected cement increase the risk of cement leakage, whereas its mechanical effects are equivocal: large cement volumes could threaten the adjacent vertebral body, but too little cement could fail to produce the beneficial restoration of load-sharing. Tests on isolated vertebral bodies have shown that improvements in strength and stiffness following vertebroplasty are influenced by the percentage cement fill [31-38] so smaller injection volumes may not adequately stabilise and strengthen the fractured vertebra. Evidently, the volume of injected cement is likely to have important mechanical consequences for the spine, and optimum volumes have yet to be specified. Some clinical studies report no significant association between injection volume and post-procedure pain and medication use [39-41] but it remains likely that injection volume will have a profound effect on spinal mechanics, and therefore on long-term clinical outcome.

The aim of the present study was to investigate how cement volume influences the three important parameters discussed above: cement leakage, distributions of compressive stress on the fractured and adjacent vertebral bodies, and load-sharing between the fractured vertebral body and its neural arch. Spinal stiffness in bending and compression were also measured to provide comparisons with previous studies. We hypothesise that high cement volumes can have both adverse and beneficial mechanical consequences, so that optimum cement volume may have to be decided separately for each individual spine.

**Materials and methods**

*Cadaveric specimens*  Thirteen thoracolumbar spines were obtained from cadavers donated for medical research. There were 6 male and 7 female spines, aged 42-91 years (mean 73 years) which were stored at -20 ºC in sealed bags until required for testing. Spines were subsequently thawed at 3 ºC, and each was dissected to provide one or more "motion segments" consisting of two adjacent vertebrae with the intervening intervertebral disc and ligaments intact.  Nineteen motion segments between T7 and L4 were obtained for the present study.  The choice of level was determined by the need to avoid large osteophytes (which interfere with disc stress measurement) and the need to maximise use of scarce human tissue.  Each motion segment was radiographed in the sagittal plane and bone mineral content (BMC) and density (BMD) of the vertebrae were measured using dual energy x-ray absorptiomety (DEXA) as described previously [26].  Further radiographs were taken after fracture to identify the fractured vertebra that was to receive vertebroplasty.  At the end of the experiment, discs were sectioned in the transverse plane and the grade of disc degeneration determined by visual inspection, using points 1 (non-degenerated) to 4 (severely degenerated) on the scale defined by Adams et al. [42].  Specimen details are shown in Table 1.

*Overview of experiments*  Each motion segment was compressed until one of the vertebral bodies fractured, and then vertebroplasty was performed twice, using 3.5cm$^3$ of PMMA each time.  (1 cm$^3$ = 1ml.)  Before and after each intervention, the following mechanical properties were evaluated: compressive and bending stiffness of the motion segment, the distribution of compressive stress within the adjacent intervertebral disc, and compressive loading on the neural arch.  Measurements were repeated a final time following a period of creep loading designed to encourage cement consolidation and to simulate loading in life.  Throughout the testing protocol, angles of flexion and extension for each specimen were measured relative to its initial neutral (unloaded) position.

3

*Mechanical testing apparatus*  Each motion segment was secured in two cups of dental plaster (Ultrahard Die Stone Iso-Type IV, Kerr S.p.A, Italy) and loaded on a computer-controlled, hydraulic materials testing machine (Dartec-Zwick-Roell, Leominster, UK).  The testing rig (Figure 1) allowed complex loading to be applied in bending and compression by means of one or two low-friction rollers.  Two rollers were used to compress the specimen while positioned at a constant angle of flexion or extension.  One roller, offset to the centre of rotation, was used to apply a physiologically-reasonable combination of bending and compression in order to simulate spinal bending movements in-vivo [43].

*Preliminary creep test*  An initial "creep" test (1.0 kN compression applied for 1 hr) was performed to simulate the diurnal change in intervertebral disc water content and height that occurs in life [44], and to ensure that disc hydration was brought within the physiological range[43].

*Compressive and bending stiffness*  Each motion segment was positioned in 2º of flexion (to simulate a slightly stooped posture that disengages the neural arches) and compressed at 600 N/s up to a maximum compressive load of 1.2 kN or 1.5 kN (depending on specimen size and BMD).  Compressive stiffness was defined as the slope of the load-deformation curve at 1 kN. To determine bending stiffness, an off-centre compressive force was applied to a single low-friction roller (Figure 1) as described previously [43].  Rotation of the upper vertebra was measured by attaching 5 mm diameter reflective markers to the apparatus and to pins inserted into the vertebral bodies.  The position of each marker was tracked at 50 Hz using a MacReflex 2D infra-red motion analysis system (Qualisys, Goteborg, Sweden) with an in-plane accuracy of approximately 5 µm which allows accurate measurements of vertebral rotations[43].  Bending moment acting on the specimen was calculated by multiplying the applied compressive force (measured by the Dartec load cell) by its lever arm (determined as the perpendicular distance between the centre of the roller applying the force and the

4

geometric centre of the disc).  Bending moment-rotation angle graphs were then plotted, and

bending stiffness was defined as the gradient of the tangent to the linear region of the graph at

4 Nm [26].

*Stress profilometry and compressive load-sharing*  A miniature pressure transducer (Gaeltec,

Dunvegan, Scotland), side-mounted in a 1.3-mm diameter needle, was used to measure the

distribution of compressive "stress" inside the intervertebral disc.  Validation tests have

shown that transducer output within disc tissues is approximately equal to the average axial

compressive stress acting perpendicular to its membrane [45-47].  The needle was pulled through

the mid-sagittal diameter of the disc while the motion segment was subjected to a

compressive force between 0.75 kN and 1.5 kN, depending upon specimen size and BMD [26, 48].  Vertical and horizontal stresses were measured in successive tests with the transducer

membrane facing vertically and then horizontally.  Profiles were obtained with the specimen

positioned in 2º of extension, to simulate the erect standing posture [49], and in 2-6º of flexion

(depending on specimen mobility) to simulate a slightly stooped posture.  Stress profiles

(Figure 1) indicated the intradiscal pressure (IDP), defined as the average pressure in the

nucleus (where vertical and horizontal stresses are equal), and the magnitude of any anterior

($SP_A$) or posterior ($SP_P$) stress peaks, calculated by subtracting IDP from the maximum stress

in the anterior and posterior annulus, respectively [26].  All data were then normalised to the 1.5

kN loading condition [47, 50].  "Integration" of the stress profiles allowed the compressive force

acting on the anterior ($F_A$) and posterior halves ($F_P$) of the disc (and vertebral body) to be

estimated [47].  Subtracting $F_A$ and $F_P$ from the applied 1.5 kN indicated the compressive force

resisted by the neural arch, which was expressed as a % ($F_N$) of the applied 1.5 kN.

*Vertebral fracture*  Each motion segment was positioned in flexion (2-10º depending on

spinal level and flexibility), to simulate a forward stooped posture.  This was achieved by

reducing the height of the rear roller (Figure 1) so that the specimen would flex forwards

5

about its own natural centre of rotation until the second roller made contact. The specimen was then compressed at a rate of 3 mm/s. This testing position ensured that most of the applied load was resisted by the disc and vertebral body, as indicated by the low level of neural arch load-bearing in flexion (Table 2). A load-deformation graph plotted in real-time allowed the load to be removed at the first sign of failure, when the curve became non-linear. The yield point at which fracture occurred was identified by the first reduction in gradient (stiffness), and the load at this point indicated the "yield strength". Fracture was confirmed, and the site of fracture determined, by comparing radiographs taken before and after overload. The severity of fracture was quantified by measuring the permanent height lost by the motion segment under a nominal load of 1kN. Subsequent mechanical loading was performed using the same angles of flexion and extension as those used before fracture, so that direct comparisons could be made between load-distributions before and after fracture, and after vertebroplasty.

*Vertebroplasty* Two 10 G vertebroplasty needles were gently tapped into the fractured vertebra by the transpedicular route, one needle being introduced through each pedicle. Sagittal plane radiographs were used to indicate when the tips of the needles were in the anterior/inferior quadrant of the vertebral body, and frontal plane radiographs indicated when both needle tips were located in the mid-sagittal region of the vertebral body, away from the lateral margins, as recommended in clinical practice [40]. For each injection (VP1 or VP2), PMMA cement (Spineplex®, Stryker Instruments, Howmedica International, Limerick, Ireland) was prepared by mixing 10 g of powder with 5 cm$^3$ of monomer liquid. In VP1, 3.5cm$^3$ of cement was injected unipedicularly through a single needle while the other needle remained in position to ensure that cement did not flow down the needle track in the bone. Both needles were then removed from the vertebra and the cement was left to set for 1 h before another radiograph was taken to confirm the placement of cement and any leakage.

VP2 was performed in an identical manner by injecting a further $3.5cm^3$ of cement via the other pedicle, after re-inserting the second needle. Further radiographs were taken to confirm the final placement of cement and any additional leakage. Cement leakage was quantified after each injection by collecting the fragments of cement that had leaked from the vertebral body, and measuring their combined volume by immersing them in water. After VP2, the motion segment was compressed for a further 1h at 1.0 kN to allow cement consolidation. All mechanical tests were performed before fracture (following the initial creep test), after fracture, after each cement injection, and after consolidation. Predicted % fill of the vertebral body with cement following each injection was calculated by expressing the injected volume ($3.5cm^3$ or $7.0cm^3$) as a percentage of the vertebral body volume. Volume was determined by water immersion following removal of the neural arch and adjacent disc after testing. The actual % fill following each injection was similarly determined after subtracting the volume of any leaked cement from the injected volume.

*Statistical analysis* Repeated measures analysis of variance (ANOVA) was used to compare measurements across five consecutive time points (pre-fracture, post-fracture, post-VP1, post-VP2, and post-consolidation). Where a significant main effect was found, post-hoc paired comparisons were employed to identify where the differences arose. Pearson's Chi-square test was used to compare the effects of gender and spinal level (thoracic or lumbar) on the incidence of cement leakage. Group t-tests were used to compare vertebral body volume and % fill in specimens with and without leakage. Linear regression and Pearson's correlation coefficient were used to compare leakage volume with vertebral body volume, and to compare % fill with the mechanical parameters following vertebroplasty. In all tests, $p<0.05$ was considered significant. SPSS 14.0® was used for all statistical analyses. Values shown are the mean ± standard deviation, unless stated otherwise.

**Results**

*Vertebral fracture* Yield strengths ranged from 1.3 - 5.2 kN (Table 1) and average motion segment height loss was $2.47 \pm 0.37$ mm. Radiographs showed that 14/19 specimens failed in the lower vertebral body and five failed in the upper vertebral body. Fracture typically involved the anterior vertebral body and the end plate adjacent to the disc, and resembled common types of fracture seen in patients with osteoporosis [51-53]. Greater height loss can be observed clinically [54] probably because, during a traumatic event, it would be difficult to remove the compressive load as soon as damage was initiated.

*Vertebroplasty* The first and second vertebroplasty procedures (VP1 and VP2) were successfully completed in all 19 motion segments (Figure 2). Cement leakage was observed in 3 specimens during VP1 and in 7 during VP2 (Table 1). Leakage volume was greater during VP2 than VP1 (averaging 1.57 cm$^3$ and 0.67 cm$^3$ respectively), and total leakage following VP2 was inversely related to vertebral body volume (r=0.47, p=0.04). The incidence of leakage was greater in thoracic compared to lumbar vertebrae (p=0.047) and in female compared to male specimens (p=0.048). Furthermore, vertebral bodies that leaked (Table 1) had smaller volumes than those that did not (20.9±7.9 cm$^3$ vs 39.5±18.1 cm$^3$ respectively, p=0.02) and hence their predicted % fill was greater (37.7±13.6 % vs 22.4±12.3 % respectively following VP2, p=0.02).

*Compressive and bending stiffness* Bending stiffness was not assessed after cement consolidation, and bending stiffness data following VP2 was lost for specimen 17 and was not obtained for specimens 5 and 8 because of concerns about damaging these particularly small and frail specimens. Fracture reduced bending stiffness by 37% and compressive stiffness by 50% (Table 2). VP1 increased bending and compressive stiffness by a small amount, but significant increases were observed only after VP2. The increase in compressive

8

stiffness following VP2 was related to the actual % fill of the vertebral body after taking into account any leakage (r=0.47, p=0.044).

*Stress profilometry* Vertebral fracture reduced IDP by 59% in flexion and 85% in extension (Figure 3). Stress peaks in the posterior annulus ($SP_P$) increased by 362% in flexion and 107% in extension (Figure 4). These changes were significantly reversed following VP1, and in all cases, parameters were restored to pre-fracture values, except for IDP (in extension) which was only partially restored. No further changes in IDP or $SP_P$ were observed following VP2 or creep consolidation. $SP_A$ was not significantly affected by fracture, VP1 or VP2. Increases in IDP following VP1 were correlated to the actual % fill of the vertebral body in both flexion (r=0.56, p=0.01) and extension (r=0.53, p=0.02), and these correlations were strengthened after VP2 in flexion (r=0.69, p=0.001) and extension (r=0.85, p<0.001).

"Stress integration" showed that vertebral fracture reduced the compressive load resisted by the anterior half of the disc and vertebral body ($F_A$) by 59% in flexion and by 60% in extension (data calculated from Table 2). Fracture also reduced the compressive load resisted by the posterior half of the disc and vertebral body ($F_P$) by 27% in extension. Reduced load-bearing by the disc after fracture lead to greater load-bearing by the neural arch ($F_N$), which increased from 11% to 39% of the applied load in flexion, and from 33% to 59% of the applied load in extension. VP1 partially and significantly restored $F_A$ towards pre-fracture values in both flexion and extension, but neither VP2 nor creep consolidation caused any further change. In contrast, $F_P$ was further and significantly decreased by VP1, but this was partially reversed by VP2 which significantly increased $F_P$. Neural arch load-bearing ($F_N$) was largely unaffected by VP1 but was reduced towards pre-fracture values (in both flexion and extension) following VP2. Creep consolidation increased $F_N$ slightly, as reported previously [25, 26].

9

**Discussion**

*Summary of findings* Following vertebral fracture, motion segment stiffness in compression and bending, intradiscal pressure (IDP) in the adjacent disc, and load-bearing by the anterior disc and vertebral body ($F_A$) were all reduced whereas stress peaks in the posterior annulus ($SP_P$), and compressive load-bearing by the neural arch ($F_N$), were increased. Vertebroplasty involving 3.5cm$^3$ of PMMA partially restored IDP, $SP_P$, and $F_A$ towards pre-fracture values. An additional 3.5 cm$^3$ of PMMA produced no further improvements in these parameters, but it partially restored motion segment stiffness in compression and bending, and $F_N$, towards pre-fracture values. Following the second cement injection, the incidence of cement leakage more than doubled, as did the average leakage volume. Leakage incidence and volume were greater in specimens with smaller vertebral bodies, and those specimens with the greatest % fill of cement also showed greater increases in IDP and compressive stiffness following vertebroplasty.

*Strengths and weaknesses of the study* A major strength of the study is the use of human spine specimens (including the neural arch and intervertebral disc) which comprise a better model of the clinical situation than animal tissues or isolated vertebral bodies (or mathematical models based on either of these). Also, the use of repeated interventions (VP1, and VP2) on the same specimens enabled the influence of cement volume to be analysed while minimising the influence of confounding variables such as BMD, disc degeneration, age, and gender [26]. Complex loading applied in the experiments reflects as closely as possible the loads experienced in-vivo [55], and vertebral fractures were obtained, as in life, by excessive mechanical loading applied to the vertebral body by its adjacent disc. The techniques of "stress profilometry" and "stress integration" have been extensively validated [45-47] and provide a straightforward means of quantifying how load is distributed on the vertebral body, the neural arch, and adjacent vertebrae. Weaknesses of the study include

frozen storage of cadaveric tissues (which alters slightly some mechanical properties of spinal tissues [56]) and analysing vertebral movements only in the sagittal plane. The use of short segments of spine may alter the load-bearing response compared to the in-vivo situation. In this study, attempts were made to tailor the bending and compressive loads during testing to accommodate differences in specimen strength and flexibility. However, the loading conditions may still differ from those experienced by the intact spine in life.

*Relationship to other studies* Cement volumes used in the present study are similar, and produced similar effects, to those used previously. Experiments on isolated cadaver vertebral bodies showed that strength can be restored to pre-fracture values using as little as 2 cm$^3$ of PMMA cement, [31] but full restoration of vertebral body stiffness required injection volumes of approximately 4 cm$^3$ in thoracic vertebrae and 6-8 cm$^3$ in thoracolumbar and lumbar vertebrae [31, 37, 38]. In our own previous studies, bi-pedicular injection of 7 cm$^3$ of PMMA was generally insufficient to restore fully the bending and compressive stiffness of intact motion segments, whereas intradiscal pressure, and stress peaks in the posterior annulus, were usually restored to near their pre-fracture values [25, 26]. The effects of vertebral fracture on intradiscal stresses and neural arch load-bearing also agree with previous studies from our own [23-26] and other [57] laboratories, and the effects of vertebroplasty measured here agree with the predictions of mathematical models [27, 28].

*Explanation of results* The most important finding of the present study is that only a small volume of cement (13% fill, on average) is required to equalise stress distributions acting on the fractured and adjacent vertebral bodies, and yet larger cement volumes (25% fill, on average) are required to restore compressive load-sharing between the anterior and posterior columns. This can be explained with the help of Figure 5. Most types of vertebral fracture involve damage to an endplate or its supporting trabeculae. The endplate can then bulge into the vertebral body when the spine is compressed, increasing the space available for the disc

11

nucleus and therefore causing pressure within the nucleus to drop. Compressive load-bearing is transferred to the annulus, increasing stress concentrations within it [24, 26], especially posterior to the nucleus where most thoracolumbar discs are thinnest (Figure 5B). Increased radial bulging of the annulus reduces disc height, and allows the neural arch to become grossly weight-bearing, especially in extended postures [24, 47]. Injecting a small volume of cement into the vertebral body (VP1) can prevent excessive deflection of the endplate under load, and this is sufficient to increase IDP and restore normal stress distributions within the disc (Figure 5C). However, damage to trabecular bone supporting the endplate is not fully stabilised, and the vertebral body continues to deform more than normal under load, ensuring that neural arch load-bearing remains elevated. Only when extra cement is injected (VP2) is the stiffness of the whole vertebral body restored, so that load-sharing between body and neural arch can return close to normal (Figure 5D). This also explains why compressive stiffness was substantially increased only following VP2. The increase in stiffness after VP2 showed some dependence on % fill of the vertebral body, but this relationship was not significant after VP1, and even after VP2 was weaker than that observed for IDP. Other factors may influence the increase in compressive stiffness following vertebroplasty, including the materials properties and placement of the injected cement, the severity of fracture, and vertebral BMD.

Stiffness in bending is reduced by fracture because motion segment height loss creates slack in the intervertebral ligaments [43], and bending stiffness is increased only after VP2 has restored the vertebral body's compressive stiffness so that it does not deform excessively when loaded. In the present study, 7cm$^3$ of PMMA (VP2) did not fully restore motion segment stiffness in compression and bending, although 7cm$^3$ is sufficient to restore compressive stiffness to isolated lower thoracic and lumbar vertebral bodies [33, 38] This

12

discrepancy could be due to cement leakage in the present study, and the absence of intervertebral discs in the previous ones.

*Clinical implications* When treating vertebral compression fractures, the main aim of vertebroplasty is to stabilise the fracture and alleviate pain, with minimal risk of complications to the patient. Unfortunately, the results of the present study do not provide a simple means of achieving this objective by choosing a particular volume (or % fill) of cement. The main effect of increased cement volume is to remove compressive loading from the neural arch and restore it to the anterior column of discs and vertebral bodies. This could be an advantage if a patient's back pain arises from high load-bearing (and consequent osteoarthritis [58]) in the apophyseal joints. However, in a patient with severe osteoporosis, a high cement volume could overload the anterior column when the spine is flexed, because the anterior region of the vertebral body becomes disproportionately weak in such patients [59]. If a patient's pain is suspected to be due to micromovement of fractured trabeculae, then it may be preferable to inject a greater volume, or to better target the cement at the damaged trabeculae. Another possibility is that the patient's pain arises from sensitised nerves in the outer posterior annulus, which is innervated by nociceptive nerve endings [60][61]. In such a case, only 3.5 cm$^3$ of cement (approximately 13% fill) could be sufficient to remove high stress concentrations from the posterior annulus and alleviate the pain. In the present study, this volume of cement was also sufficient to restore intradiscal pressure without elevating it to such high levels that it threatened the adjacent level.

In this cadaveric study, cement leakage was greater after the second cement injection, which increased the percentage fill to 25% on average. However, the elapsed time between the two injections would have allowed the first bolus of cement to set before the second was introduced, and this would not occur in clinical usage. This artefact could have obstructed or altered the flow of cement during the second injection, contributing to increased leakage.

13

However, the greater incidence of leakage at thoracic levels and in female spines, <u>as well as</u> <u>the greater volume of leakage observed in specimens with smaller vertebral bodies,</u> suggest that higher volumetric fills probably contribute to an increased risk of cement leakage *in vivo*.

*Unanswered questions and future research*  The results of the present study support our hypothesis: they show that increasing cement volume produces complex effects on spine mechanics that could be beneficial in one spine but potentially harmful in another.  Further work is required to a) develop techniques to identify the source of pain in individual patients with vertebral fractures, and b) relate pain relief following vertebroplasty to cement volume (expressed as % volumetric fill) in different groups of patients.  It is also worth considering how the *placement* of cement (rather than its volume) can affect spine mechanics and clinical outcome.  Improved placement of cement may help to avoid transferring too much load on to the anterior column and in doing so may prevent excessive endplate deformation and its sequelae in the adjacent vertebra.

14

**Figure Legends**

**Figure 1.** Apparatus used for mechanical testing of cadaver spine motion segments. The height of the rollers was adjusted so that the specimen was compressed at the desired flexion/extension angle. The posterior roller was removed altogether for tests of bending stiffness. Stress profilometry was performed by pulling a pressure transducer along the mid-sagittal diameter of the loaded disc. A typical stress profile demonstrates how IDP, $SP_A$, and $SP_P$ were measured. (A: anterior; P: posterior.)

**Figure 2.** Lateral radiograph of a specimen (Male 66, L3-4) showing the upper vertebral body (UVB), intervertebral disc (IVD), and the filling of the lower vertebral body (LVB) with cement (C) following the first (Fig 2A) and second (Fig 2B) injection of $3.5cm^3$ of PMMA cement. Pins inserted into the vertebral body carried reflective markers that were used to track angular movements for the assessment of bending stiffness.

**Figure 3.** Intradiscal pressure (IDP) at different stages of the experiment procedure. Mean values are shown. Error bars indicate the SEM. Significant difference from pre-fracture (*) and post-fracture (†) values are indicated.

**Figure 4.** Posterior stress peaks ($SP_P$) at different stages of the experiment procedure. Mean values are shown. Error bars indicate the SEM. Significant difference from pre-fracture (*) and post-fracture (†) values are indicated.

**Figure 5.** Diagram summarising the changes in load-bearing by vertebrae: A) before fracture, B) after fracture, C) after VP1, and D) after VP2. The length of the upward pointing arrows represents relative load-bearing in different regions of the vertebra. See text for details.

**References**

1.      Deramond H, Depriester C, Galibert P, Le Gars D. Percutaneous vertebroplasty with polymethylmethacrylate. Technique, indications, and results. Radiol Clin North Am 1998;36(3):533-46.

2.      Barr JD, Barr MS, Lemley TJ, McCann RM. Percutaneous vertebroplasty for pain relief and spinal stabilization. Spine 2000;25(8):923-8.

3.      Diamond TH, Champion B, Clark WA. Management of acute osteoporotic vertebral fractures: a nonrandomized trial comparing percutaneous vertebroplasty with conservative therapy. Am J Med 2003;114(4):257-65.

4.      Diamond TH, Bryant C, Browne L, Clark WA. Clinical outcomes after acute osteoporotic vertebral fractures: a 2-year non-randomised trial comparing percutaneous vertebroplasty with conservative therapy. Med J Aust 2006;184(3):113-7.

5.      Heini PF, Walchli B, Berlemann U. Percutaneous transpedicular vertebroplasty with PMMA: operative technique and early results. A prospective study for the treatment of osteoporotic compression fractures. Eur Spine J 2000;9(5):445-50.

6.      Hochmuth K, Proschek D, Schwarz W, Mack M, Kurth AA, Vogl TJ. Percutaneous vertebroplasty in the therapy of osteoporotic vertebral compression fractures: a critical review. Eur Radiol 2006;16(5):998-1004.

7.      Caudana R, Renzi Brivio L, Ventura L, Aitini E, Rozzanigo U, Barai G. CT-guided percutaneous vertebroplasty: personal experience in the treatment of osteoporotic fractures and dorsolumbar metastases. Radiol Med (Torino) 2008;113(1):114-33.

8.      Bhatia C, Barzilay Y, Krishna M, Friesem T, Pollock R. Cement leakage in percutaneous vertebroplasty: effect of preinjection gelfoam embolization. Spine 2006;31(8):915-9.

9.      Mousavi P, Roth S, Finkelstein J, Cheung G, Whyne C. Volumetric quantification of cement leakage following percutaneous vertebroplasty in metastatic and osteoporotic vertebrae. J Neurosurg 2003;99(1 Suppl):56-9.

10.     Ryu KS, Park CK, Kim MC, Kang JK. Dose-dependent epidural leakage of polymethylmethacrylate after percutaneous vertebroplasty in patients with osteoporotic vertebral compression fractures. J Neurosurg 2002;96(1 Suppl):56-61.

11.     Baroud G, Crookshank M, Bohner M. High-viscosity cement significantly enhances uniformity of cement filling in vertebroplasty: an experimental model and study on cement leakage. Spine 2006;31(22):2562-8.

12.     Loeffel M, Ferguson SJ, Nolte LP, Kowal JH. Vertebroplasty: experimental characterization of polymethylmethacrylate bone cement spreading as a function of viscosity, bone porosity, and flow rate. Spine 2008;33(12):1352-9.

13.     Luginbuhl M. Percutaneous vertebroplasty, kyphoplasty and lordoplasty: implications for the anesthesiologist. Current opinion in anaesthesiology 2008;21(4):504-13.

14.     Baroud G, Steffen T. A new cannula to ease cement injection during vertebroplasty. Eur Spine J 2005;14(5):474-9.

15.     Lee BJ, Lee SR, Yoo TY. Paraplegia as a complication of percutaneous vertebroplasty with polymethylmethacrylate: a case report. Spine 2002;27(19):E419-22.

16.     Chen HL, Wong CS, Ho ST, Chang FL, Hsu CH, Wu CT. A lethal pulmonary embolism during percutaneous vertebroplasty. Anesthesia and analgesia 2002;95(4):1060-2, table of contents.

17.     Padovani B, Kasriel O, Brunner P, Peretti-Viton P. Pulmonary embolism caused by acrylic cement: a rare complication of percutaneous vertebroplasty. AJNR Am J Neuroradiol 1999;20(3):375-7.

18.     Komemushi A, Tanigawa N, Kariya S, et al. Percutaneous vertebroplasty for osteoporotic compression fracture: multivariate study of predictors of new vertebral body fracture. Cardiovasc Intervent Radiol 2006;29(4):580-5.

19.     Tanigawa N, Komemushi A, Kariya S, Kojima H, Shomura Y, Sawada S. Radiological follow-up of new compression fractures following percutaneous vertebroplasty. Cardiovasc Intervent Radiol 2006;29(1):92-6.

20.     Trout AT, Kallmes DF, Kaufmann TJ. New fractures after vertebroplasty: adjacent fractures occur significantly sooner. AJNR Am J Neuroradiol 2006;27(1):217-23.

21.     Trout AT, Kallmes DF, Layton KF, Thielen KR, Hentz JG. Vertebral endplate fractures: an indicator of the abnormal forces generated in the spine after vertebroplasty. J Bone Miner Res 2006;21(11):1797-802.

22.     Uppin AA, Hirsch JA, Centenera LV, Pfiefer BA, Pazianos AG, Choi IS. Occurrence of new vertebral body fracture after percutaneous vertebroplasty in patients with osteoporosis. Radiology 2003;226(1):119-24.

23.     Adams MA, McNally DS, Wagstaff J, Goodship AE. Abnormal stress concentrations in lumbar intervertebral discs following damage to the vertebral body: a cause of disc failure. Eur Spine J 1993;1:214-21.

24.     Adams MA, Freeman BJ, Morrison HP, Nelson IW, Dolan P. Mechanical initiation of intervertebral disc degeneration. Spine 2000;25(13):1625-36.

25.     Farooq N, Park JC, Pollintine P, Annesley-Williams DJ, Dolan P. Can vertebroplasty restore normal load-bearing to fractured vertebrae? Spine 2005;30(15):1723-30.

26.     Luo J, Skrzypiec DM, Pollintine P, Adams MA, Annesley-Williams DJ, Dolan P. Mechanical efficacy of vertebroplasty: Influence of cement type, BMD, fracture severity, and disc degeneration. Bone 2007;40(4):1110-9.

27.     Baroud G, Nemes J, Heini P, Steffen T. Load shift of the intervertebral disc after a vertebroplasty: a finite-element study. Eur Spine J 2003.

28.     Polikeit A, Nolte LP, Ferguson SJ. The effect of cement augmentation on the load transfer in an osteoporotic functional spinal unit: finite-element analysis. Spine 2003;28(10):991-6.

29.     Ahn Y, Lee JH, Lee HY, Lee SH, Keem SH. Predictive factors for subsequent vertebral fracture after percutaneous vertebroplasty. J Neurosurg Spine 2008;9(2):129-36.

30.     Lin EP, Ekholm S, Hiwatashi A, Westesson PL. Vertebroplasty: cement leakage into the disc increases the risk of new fracture of adjacent vertebral body. AJNR Am J Neuroradiol 2004;25(2):175-80.

31.     Belkoff SM, Mathis JM, Jasper LE, Deramond H. The biomechanics of vertebroplasty. The effect of cement volume on mechanical behavior. Spine 2001;26(14):1537-41.

32.     Dean JR, Ison KT, Gishen P. The strengthening effect of percutaneous vertebroplasty. Clin Radiol 2000;55(6):471-6.

33.     Graham J, Ahn C, Hai N, Buch BD. Effect of bone density on vertebral strength and stiffness after percutaneous vertebroplasty. Spine 2007;32(18):E505-11.

34.     Higgins KB, Harten RD, Langrana NA, Reiter MF. Biomechanical effects of unipedicular vertebroplasty on intact vertebrae. Spine 2003;28(14):1540-7; discussion 8.

35.     Liebschner MA, Rosenberg WS, Keaveny TM. Effects of bone cement volume and distribution on vertebral stiffness after vertebroplasty. Spine 2001;26(14):1547-54.

36.     Molloy S, Mathis JM, Belkoff SM. The effect of vertebral body percentage fill on mechanical behavior during percutaneous vertebroplasty. Spine 2003;28(14):1549-54.

37.	Tohmeh AG, Mathis JM, Fenton DC, Levine AM, Belkoff SM. Biomechanical efficacy of unipedicular versus bipedicular vertebroplasty for the management of osteoporotic compression fractures. Spine 1999;24(17):1772-6.

38.	Molloy S, Riley LH, 3rd, Belkoff SM. Effect of cement volume and placement on mechanical-property restoration resulting from vertebroplasty. AJNR Am J Neuroradiol 2005;26(2):401-4.

39.	Cotten A, Dewatre F, Cortet B, et al. Percutaneous vertebroplasty for osteolytic metastases and myeloma: effects of the percentage of lesion filling and the leakage of methyl methacrylate at clinical follow-up. Radiology 1996;200(2):525-30.

40.	Jensen ME, Evans AJ, Mathis JM, Kallmes DF, Cloft HJ, Dion JE. Percutaneous polymethylmethacrylate vertebroplasty in the treatment of osteoporotic vertebral body compression fractures: technical aspects. AJNR Am J Neuroradiol 1997;18(10):1897-904.

41.	Kaufmann TJ, Trout AT, Kallmes DF. The effects of cement volume on clinical outcomes of percutaneous vertebroplasty. AJNR Am J Neuroradiol 2006;27(9):1933-7.

42.	Adams MA, Dolan P, Hutton WC. The stages of disc degeneration as revealed by discograms. J Bone Joint Surg [Br] 1986;68(1):36-41.

43.	Zhao F, Pollintine P, Hole BD, Dolan P, Adams MA. Discogenic origins of spinal instability. Spine 2005;30(23):2621-30.

44.	Botsford DJ, Esses SI, Ogilvie-Harris DJ. In vivo diurnal variation in intervertebral disc volume and morphology. Spine 1994;19(8):935-40.

45.	Chu JY, Skrzypiec D, Pollintine P, Adams MA. Can compressive stress be measured experimentally within the annulus fibrosus of degenerated intervertebral discs? Proc Inst Mech Eng [H] 2008;222(2):161-70.

46.	McNally DS, Adams MA, Goodship AE. Development and validation of a new transducer for intradiscal pressure measurement. J Biomed Eng 1992;14(6):495-8.

47.     Pollintine P, Przybyla AS, Dolan P, Adams MA. Neural arch load-bearing in old and degenerated spines. J Biomech 2004;37(2):197-204.

48.     Adams MA, McNally DS, Dolan P. 'Stress' distributions inside intervertebral discs. The effects of age and degeneration. J Bone Joint Surg Br 1996;78(6):965-72.

49.     Adams MA, Hutton WC. The effect of posture on the role of the apophysial joints in resisting intervertebral compressive forces. J Bone Joint Surg [Br] 1980;62(3):358-62.

50.     Skrzypiec DM, Pollintine P, Przybyla A, Dolan P, Adams MA. The internal mechanical properties of cervical intervertebral discs as revealed by stress profilometry. Eur Spine J 2007;16(10):1701-9.

51.     Hedlund LR, Gallagher JC, Meeger C, Stoner S. Change in vertebral shape in spinal osteoporosis. Calcif Tissue Int 1989;44(3):168-72.

52.     Oda K, Shibayama Y, Abe M, Onomura T. Morphogenesis of vertebral deformities in involutional osteoporosis. Age-related, three-dimensional trabecular structure. Spine 1998;23(9):1050-5, discussion 6.

53.     Wu CT, Lee SC, Lee ST, Chen JF. Classification of symptomatic osteoporotic compression fractures of the thoracic and lumbar spine. J Clin Neurosci 2006;13(1):31-8.

54.     Ferrar L, Jiang G, Clowes JA, Peel NF, Eastell R. Comparison of densitometric and radiographic vertebral fracture assessment using the algorithm-based qualitative (ABQ) method in postmenopausal women at low and high risk of fracture. J Bone Miner Res 2008;23(1):103-11.

55.     Dolan P, Earley M, Adams MA. Bending and compressive stresses acting on the lumbar spine during lifting activities. J Biomech 1994;27(10):1237-48.

56.     Adams MA. Mechanical testing of the spine. An appraisal of methodology, results, and conclusions. Spine 1995;20(19):2151-6.

57.     Holm S, Holm AK, Ekstrom L, Karladani A, Hansson T. Experimental disc degeneration due to endplate injury. J Spinal Disord Tech 2004;17(1):64-71.

58.     Brown KR, Pollintine P, Adams MA. Biomechanical implications of degenerative joint disease in the apophyseal joints of human thoracic and lumbar vertebrae. Am J Phys Anthropol 2008;136(3):318-26.

59.     Adams MA, Pollintine P, Tobias JH, Wakley GK, Dolan P. Intervertebral disc degeneration can predispose to anterior vertebral fractures in the thoracolumbar spine. J Bone Miner Res 2006;21(9):1409-16.

60.     Coppes MH, Marani E, Thomeer RT, Groen GJ. Innervation of "painful" lumbar discs. Spine 1997;22(20):2342-9; discussion 9-50.

61.     Kuslich SD, Ulstrom CL, Michael CJ. The tissue origin of low back pain and sciatica: a report of pain response to tissue stimulation during operations on the lumbar spine using local anesthesia. Orthop Clin North Am 1991;22(2):181-7.

**tables**

**Table 1.  Details of the 19 specimens tested**

| Gender (M/F) | Age (yrs) | Spinal level | Disc degen grade | VB vol$^+$ (cm$^3$) | BMD$^+$ (g/cm$^3$) | Yield strength (kN) | Cement leak (cm$^3$)$^{\#}$ | | % Fill (Predicted) | | % Fill (Actual) | |
|---|---|---|---|---|---|---|---|---|---|---|---|---|
| | | | | | | | VP1 | VP2 | VP1 | VP2 | VP1 | VP2 |
| F | 51 | T12-L1 | 2 | 28.0 | 0.1445 | 2.5 | | 0.5 | 12.5 | 25 | 12.5 | 23.2 |
| M | 82 | T11-12 | 4 | 34.0 | 0.1484 | 2.9 | 0.5 | 2.0 | 10.3 | 20.6 | 8.8 | 14.7 |
| F | 51 | T10-11 | 2 | 23.0 | 0.1041 | 2.1 | | | 15.2 | 30.4 | 15.2 | 30.4 |
| M | 86 | L2-3 | 4 | 66.0 | 0.3188 | 2.3 | | | 5.3 | 10.6 | 5.3 | 10.6 |
| F | 91 | T7-8 | 2 | 12.0 | 0.1321 | 1.3 | | 2.0 | 29.2 | 58.4 | 29.2 | 41.7 |
| F | 51 | T10-11 | 2 | 19.0 | 0.1589 | 2.3 | | 0.5 | 18.4 | 36.8 | 18.4 | 34.2 |
| M | 82 | T10-11 | 3 | 23.0 | 0.1181 | 3.0 | | 0.5 | 15.2 | 30.4 | 15.2 | 28.3 |
| F | 42 | T7-8 | 1 | 14.0 | 0.1491 | 1.7 | 1.0 | 2.5 | 25 | 50 | 17.9 | 32.1 |
| M | 67 | T10-11 | 3 | 30.5 | 0.1341 | 1.7 | | | 11.5 | 23 | 11.5 | 23.0 |
| F | 76 | L3-4 | 4 | 41.5 | 0.4366 | 5.2 | | | 8.4 | 16.8 | 8.4 | 16.9 |
| F | 81 | T9-10 | 3 | 16.5 | 0.1208 | 1.8 | 0.5 | 3.0 | 21.2 | 42.4 | 18.2 | 24.2 |
| M | 82 | T7-8 | 3 | 20.0 | 0.1721 | 4.1 | | | 17.5 | 35 | 17.5 | 35.0 |
| F | 85 | T8-9 | 3 | 14.0 | 0.2207 | 2.7 | | | 25 | 50 | 25.0 | 50.0 |
| M | 89 | L2-3 | 3 | 68.5 | 0.1611 | 3.9 | | | 5.1 | 10.2 | 5.1 | 10.2 |
| M | 89 | T11-12 | 3 | 45.0 | 0.0874 | 2.2 | | | 7.8 | 15.6 | 7.8 | 15.6 |
| M | 66 | L3-4 | 3 | 52.0 | 0.1266 | 1.7 | | | 6.7 | 13.4 | 6.7 | 13.5 |
| M | 66 | L1-2 | 4 | 51.0 | 0.1249 | 2.4 | | | 6.9 | 13.8 | 6.9 | 13.7 |
| M | 82 | T8-9 | 3 | 21.0 | 0.0997 | 2.8 | | | 16.7 | 33.4 | 16.7 | 33.3 |
| M | 66 | T10-11 | 3 | 41.0 | 0.1099 | 1.7 | | | 8.5 | 17 | 8.5 | 17.1 |
| **Mean** | **72.9** | | | **32.6** | **0.1615** | **2.5** | **0.67** | **1.57** | **14.0** | **28.0** | **13.4** | **24.6** |
| **SD** | **15.2** | | | **17.5** | **0.0842** | **1.0** | **0.29** | **1.06** | **7.3** | **14.5** | **6.7** | **11.2** |

Note: + Vertebral body volume and BMD are shown for the fractured vertebra.
\# Blank spaces indicate no observable leak

**Table 2.** Average (SD) results at different stages of the experiment

| | Pre-fracture | Post-fracture | Post-VP1 | Post-VP2 | Post-consolidation | p |
|---|---|---|---|---|---|---|
| IDP- flex (MPa) | 1.34(1.29) | 0.55(0.64)$^{b}$ | 0.95(0.69)$^{B}$ | 1.00(0.68)$^{C}$ | 0.94(0.69)$^{B}$ | 0.002 |
| IDP- ext (MPa) | 1.39(1.18) | 0.20(0.41)$^{c}$ | 0.65(0.69)$^{cC}$ | 0.83(0.88)$^{bC}$ | 0.75(0.76)$^{cC}$ | <0.001 |
| SP$_P$ - flex (MPa) | 0.52(0.96) | 2.46(1.28)$^{c}$ | 0.77(0.68)$^{C}$ | 0.89(1.09)$^{C}$ | 0.75(1.04)$^{C}$ | <0.001 |
| SP$_P$ - ext (MPa) | 1.37(1.44) | 2.83(1.99)$^{b}$ | 1.52(1.18)$^{C}$ | 1.67(1.65)$^{A}$ | 1.51(1.37)$^{B}$ | 0.004 |
| SP$_A$ – flex (MPa) | 2.31(2.03) | 1.30(1.06) | 1.45(1.51) | 1.52(1.70) | 1.73(2.05) | 0.111 |
| SP$_A$ – ext (MPa) | 0.33(0.38) | 0.49(0.44) | 0.42(0.47) | 0.42(0.79) | 0.43(0.53) | 0.848 |
| F$_A$ - flex (%) | 54.6(17.1) | 22.2(11.4)$^{c}$ | 34.3(16.9)$^{cB}$ | 38.3(23.1)$^{bA}$ | 39.9(21.3)$^{bB}$ | <0.001 |
| F$_A$ - ext (%) | 23.2(8.12) | 9.21(5.24)$^{c}$ | 14.8(7.49)$^{cC}$ | 18.2(13.4)$^{A}$ | 15.9(10.1)$^{cA}$ | <0.001 |
| F$_P$ - flex (%) | 34.6(18.6) | 38.3(15.2) | 30.4(14.0) | 33.2(17.1) | 30.6(17.9) | 0.333 |
| F$_P$ - ext (%) | 43.5(15.7) | 31.9(17.4)$^{b}$ | 26.1(10.6)$^{cB}$ | 33.6(15.2)$^{bD}$ | 30.2(13.7)$^{c}$ | <0.001 |
| F$_N$ - flex (%) | 10.8(13.7) | 39.4(18.1)$^{c}$ | 35.3(15.5)$^{c}$ | 28.5(14.6)$^{cB}$ | 29.4(18.5)$^{c}$ | <0.001 |
| F$_N$ - ext (%) | 33.4(16.5) | 58.9(16.7)$^{c}$ | 59.2(14.1)$^{c}$ | 48.3(15.3)$^{cBD}$ | 54.1(15.8)$^{c}$ | <0.001 |
| Compressive Stiffness (kN/mm) | 3.04(1.23) | 1.52(0.44)$^{c}$ | 1.73(0.51)$^{c}$ | 1.96(0.73)$^{cB}$ | 2.08(0.75)$^{cC}$ | <0.001 |
| Bending Stiffness (Nm/deg) | 5.89(2.09) | 3.71(1.50)$^{c}$ | 4.35(1.58)$^{b}$ | 4.39(1.51)$^{bA}$ | | <0.001 |

Significance (final column) indicates main effects demonstrated by repeated measures ANOVA. Post-hoc paired comparisons indicate differences from pre-fracture ([a] $p < 0.05$; [b] $p < 0.01$; [c] $p < 0.001$), post-fracture ([A] $p < 0.05$; [B] $p < 0.01$; [C] $p < 0.001$), and post-VP1 ([D] $p<0.05$) values.
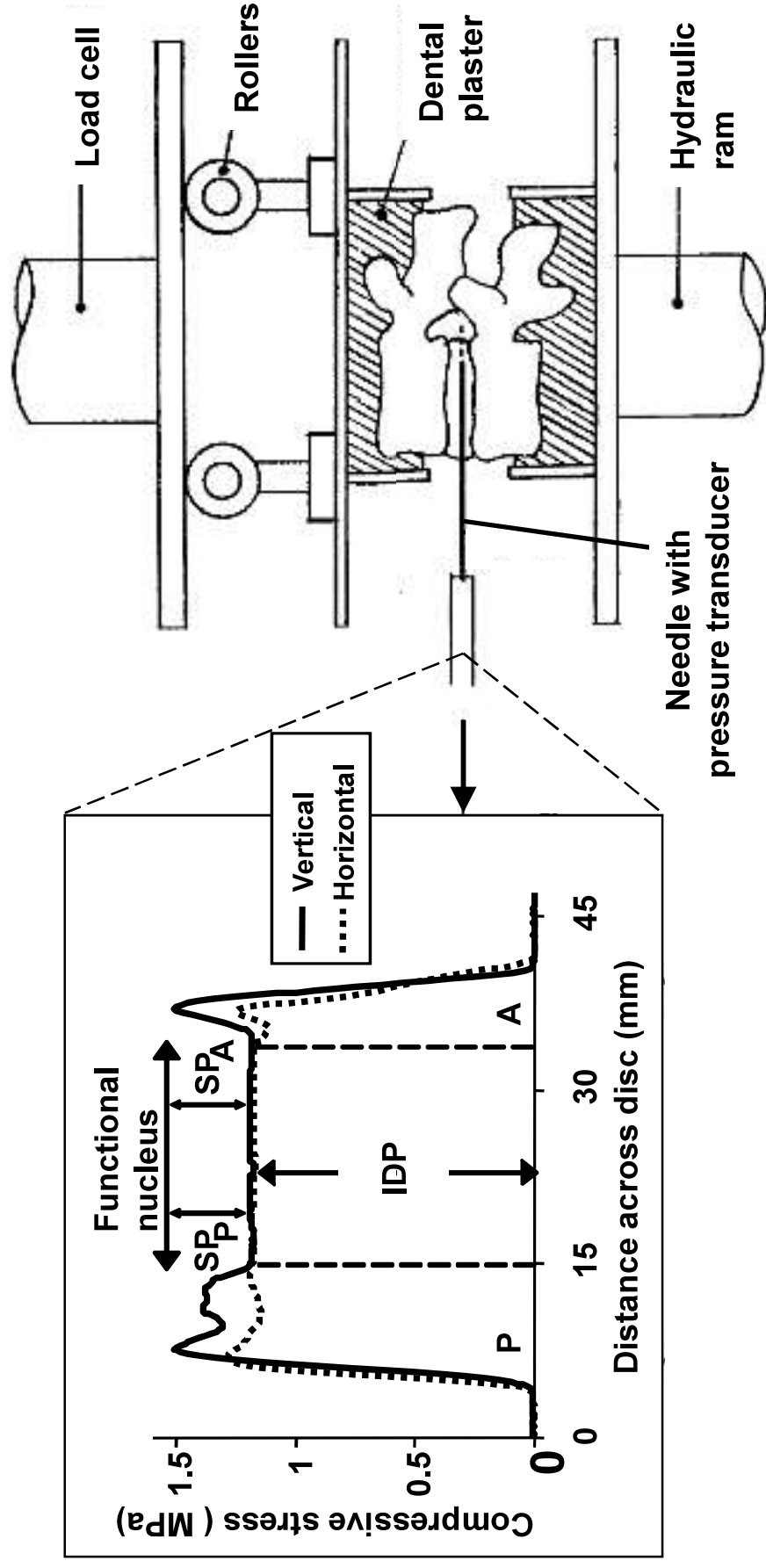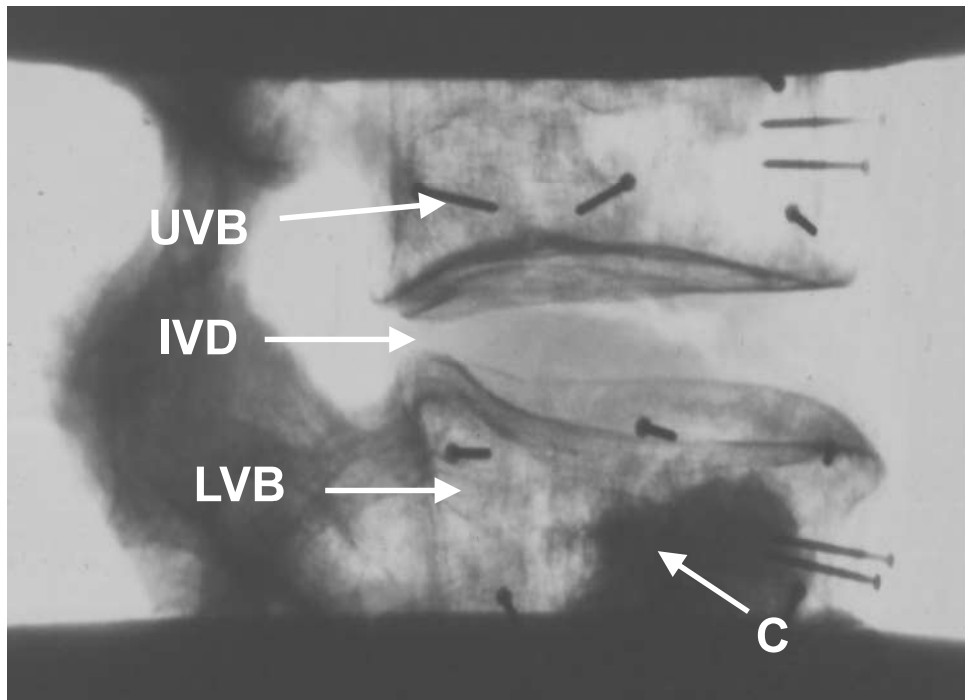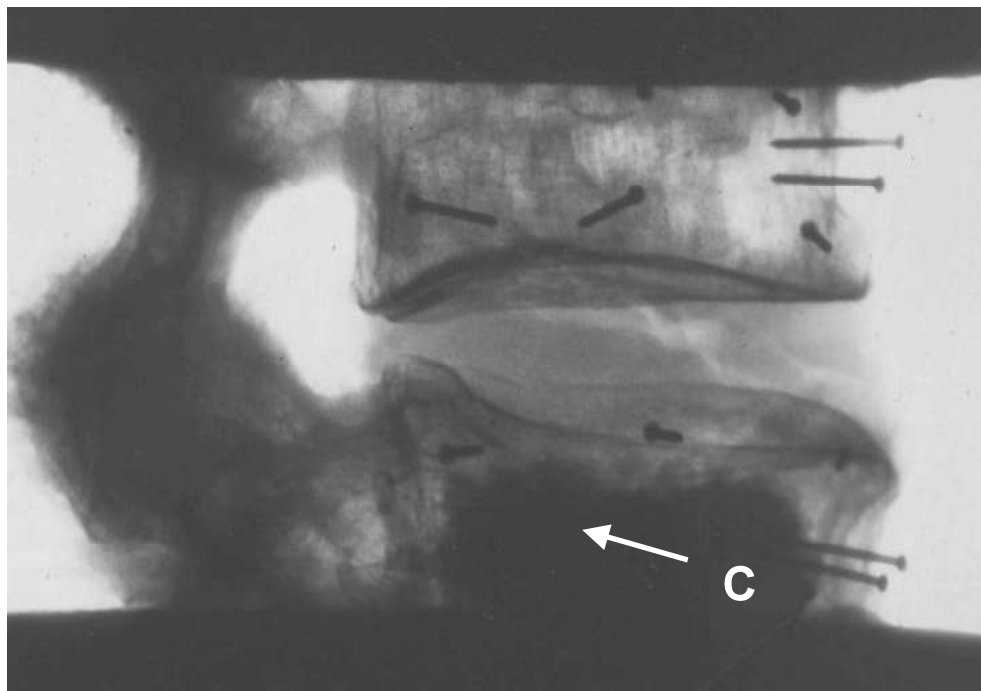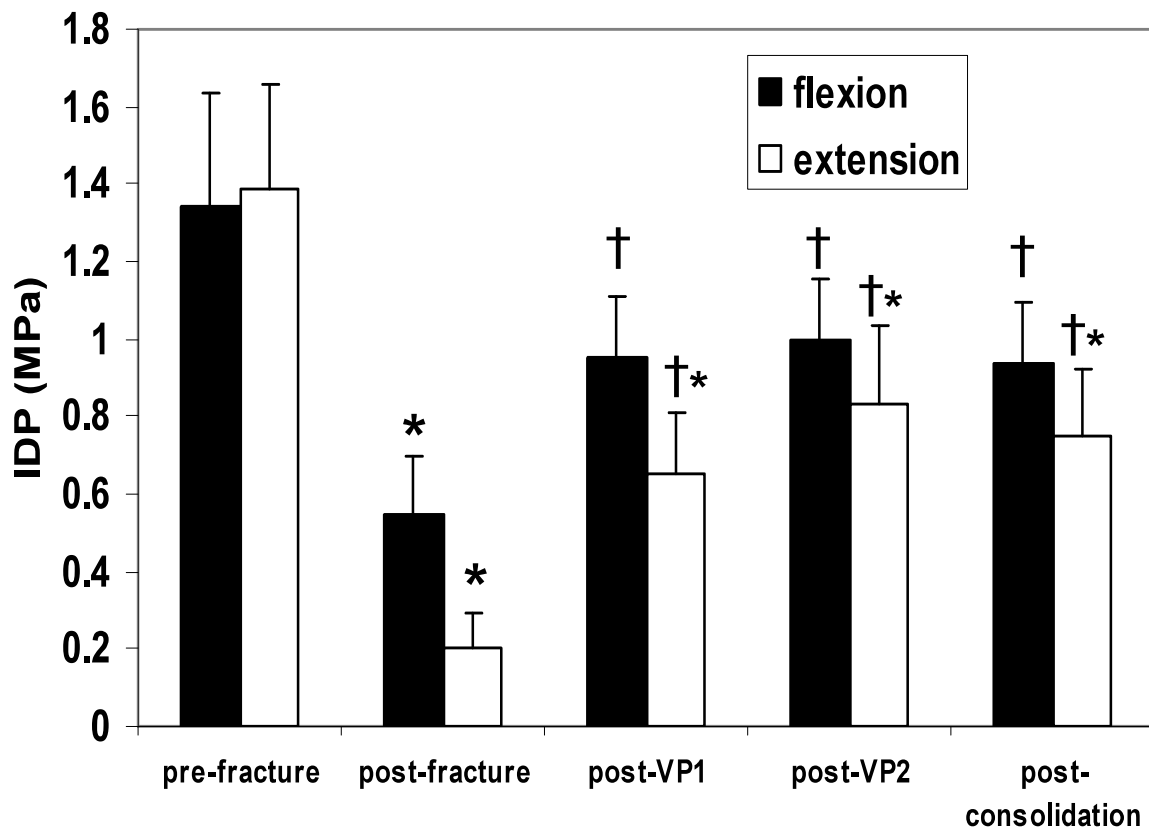
Figure 1

# Figure 1

# Figure 2A



# Figure 2B

# Figure 3

# Figure 4

Figure 5